Effect of a geometrical length scale on remanent magnetization and critical currents in Y-Ba-Cu-O and Bi-Sr-Ca-Cu-O crystals

Y. Yeshurun,* M. W. McElfresh, A. P. Malozemoff, J. Hagerhorst-Trewhella, J. Mannhart,† F. Holtzberg, and G. V. Chandrashekhar

IBM Research, Yorktown Heights, New York 10598-0218

(Received 29 November 1989; revised manuscript received 24 April 1990)

The laser ablation technique is used to grid-pattern thin Y-Ba-Cu-O and Bi-Sr-Ca-Cu-O crystals to form isolated squares of length scale R. The effect of R on irreversible magnetization and deduced critical currents is studied. The remanent magnetization ($\mathbf{H}\|\mathbf{c}$) at low temperature is linear within experimental error below a few hundred micrometers, and sublinear at larger sizes. The results are inconsistent with granularity on the scale of the twin boundaries but suggest the presence of some larger-scale defects that impede current flow. In a conventional critical-state model, a field (or flux-density) dependence of the critical current density $J_c(h) \propto h^{-n}$ gives rise to a sublinear size dependence $D^{1/(n+1)}$ of the zero-field remanent magnetization. However, in our geometry, strong demagnetizing fields are expected to curve the flux lines into the plane and reduce the size of this effect. Further evidence for the flux line curvature comes from the fact that the field for the minimum in the virgin curve is almost independent of sample size, in contrast to models that ignore the curvature.

I. INTRODUCTION

Irreversible magnetic phenomena in type-II superconductors are usually treated in the framework of the critical-state or Bean model.[1,2] This model has also been used quite frequently to explain magnetic data in high-temperature superconductors.[3–12] A simple test of the applicability of the Bean model is often based on a study of the effect of the length scale of the sample on the irreversible magnetization. For example, in the simplest version of this model, the saturation remanent magnetization of a cylindrical sample of radius R, with the field applied along the cylinder axis, is given by[1]

$$M_{\rm rem} = J_{c0} R/30 , \tag{1}$$

where J_{c0} is the critical current density assumed to be independent of field (we use J_c to stand for the critical current density in the more general field-dependent case). Exactly the same formula is appropriate for a square of side $2R$. Similarly, for a slab of thickness D, with field applied in the slab plane, the remanent magnetization is given by

$$M_{\rm rem} = J_{c0} D/40 . \tag{2}$$

Practical units, namely, A/cm^2, G, and cm, are used in Eqs. (1) and (2) and elsewhere throughout the text.

The simple scaling of $M_{\rm rem}$ with the length scale R, predicted by Eq. (1), was first demonstrated for high-temperature superconductors by Oh *et al.*[11] These authors subdivided a thin Y-Ba-Cu-O film into 4 and 16 pieces and found a linear dependence of $M_{\rm rem}$ on the length scale. Their results have recently been confirmed by McGuire *et al.*[12] who used the laser ablation technique[13] for an even finer division of a Y-Ba-C-O thin film. Conflicting results, however, are reported for crystals. Sulpice *et al.*[14] studied a set of different crystals with various sizes and found that $M_{\rm rem}$ increases sublinearly with R, with saturation at high values. They therefore concluded that the current flow is limited by intrinsic geometrical barriers inside the crystal above a length scale of about 1 mm. Some uncertainty here comes from the fact that the crystals were all different. Küpfer *et al.*[15] ground up a single crystal and measured the critical current of the resulting randomly oriented powder particles of various sizes using an ac-susceptibility technique. The irreversible magnetization which can be deduced from their $J_c R$ (R is the grain size in this case) goes up only weakly with R and fully saturates above 200 μm. They suggest a granular structure in the crystal on a scale less than 10 μm. Data on Y-Ba-Cu-O ceramics[16–18] is similarly mixed, with some data showing irreversible magnetization independent of particle size and others showing close to proportionality. The averaging over anisotropic directions makes these data hard to interpret.[9]

In this work we attempt a more controlled study of the effect of the length scale on J_c in Y-Ba-Cu-O and Bi-Sr-Ca-Cu-O crystals by varying the length scale in the *same* crystal and maintaining crystal orientation. In our experiment the subdivision of the crystal is done by laser ablation[13] in such a way that all the crystalline segments have similar size and are kept in their original orientation. We thus avoid the need for averaging length scales and orientations, which introduced uncertainties in many of the earlier experiments. We observe a steady increase of $M_{\rm rem}$ with size, which seems to rule out the possibility that twin boundaries, or any other defects on a scale smaller than 100 μm, play a role in limiting critical currents, at least at low temperatures and applied fields. However, as in one earlier study,[14] we find that $M_{\rm rem}$ is only linear up to sizes of order a few hundred microme-

ters, but becomes sublinear at larger sizes. We discuss various possible explanations for this effect in the context of the critical-state model.

This article is organized in the following way. In the next section we describe our technique for controllably cutting the crystal. We then report on results for Y-Ba-Cu-O (Sec. III) and for Bi-Sr-Ca-Cu-O (Sec. IV), and finally, in Sec. V, we discuss the results, referring to more detailed calculations of the critical-state model (with a field- or flux-density-dependent critical-current density) and the effect of demagnetization in Appendices A and B, respectively.

II. EXPERIMENTAL DATA

The details of the sample preparation are given in Refs. 19 and 20. In order to vary the length scale, we apply a micropatterning technique with an excimer laser which was originally used for thin films.[13] A variety of patterning techniques have been applied to high-temperature superconducting films, but laser ablation offers, in addition to other advantages,[13] perhaps the best resolution without noticeable degradation of T_c. Here we describe the first application of laser ablation to high-T_c *crystals*. The crystal is cemented on a flat surface of a sapphire or a phenolic rod which serves as a sample holder for laser ablation and for magnetic measurements. In the laser ablation process, the holder is mounted onto an XY stage that can be moved in the horizontal plane. A focused excimer laser beam with a wavelength of 193 nm and a pulse duration of 17 ns illuminates the sample. Typically, 100–150 pulses of uv light with a fluence of 2–4 J/cm^2 per pulse at a repetition rate of 5 Hz were used to ablate 10-μm-wide channels in (10–30)-μm-thick high-T_c crystals. An optical microscope and a scanning electron microscope (SEM) were used to detect defects on the sample which are a result of the ablation.

Magnetic measurements were made to probe the bulk properties before and after each stage of ablation. We first measured the temperature dependence of the zero-field-cooled (ZFC) magnetization M at low field. Next we measured magnetization as a function of field H (hysteresis curve). Finally, we measured relaxation rates for the ZFC magnetization and the remanent magnetization. Magnetic data were collected on commercial SQUID magnetometers (SHE for Bi-Sr-Ca-Cu-O and Quantum Design for Y-Ba-Cu-O). Field overshoot and magnetic background relaxation can be problems in the Quantum Design magnetometer, when unaccounted for. They usually manifest themselves in an artificial closing of the hysteresis curve with increasing field, as well as other anomalies. The absence of such anomalies in our data supports their reliability. A background diamagnetic signal from the substrate gives a net downward slope superimposed on the hysteresis curve.

III. Y-Ba-Cu-O

The $1300\times450\times14$ μm^3 Y-Ba-Cu-O sample undergoes a transition to a superconducting phase at $T_c=78$ K. This value is typical for Y-Ba-Cu-O crystals grown in an MgO crucible. The width of the transition in ac-susceptibility measurements is about 0.1 K. Low-field (50-Oe) dc measurements show the usual smearing of the signal at high temperatures, presumably due to flux penetration[4] above H_{c1}, with a width (20%–80%) of approximately 10 K for applied field parallel to the crystallographic c axis (perpendicular to the a-b plane) and 17 K for $\mathbf{H}\perp\mathbf{c}$. Hereafter, we refer to this crystal as the "original" one.

The original sample was ablated to form a square sample 450×450 μm^2. This square was then grid-patterned by the laser to form four isolated 175×175 μm^2 squares with 10-μm gaps between sections. (Because of the removal of several irregular pieces which were formed during the ablation, the length scale of this stage was less than half the previous one.) In the next step we obtained 16 87×87 μm^2 isolated squares, and finally, in the last stage, the sample was composed of 64 40×40 μm^2 isolated squares. An optical microscope picture of the last stage is shown in Fig. 1.

Figure 2 exhibits the ZFC magnetization, measured in $H_a=50$ Oe perpendicular to the plane, normalized to its low-temperature value, for the 1-, 4-, 16-, and 64-square samples. This figure demonstrates that the patterning has no effect on the T_c onset. The apparent effect on the width of the transition is just contrary to what one would expect from the demagnetization-enhanced flux penetration at $H_{c1}(T)$, which was observed in an earlier study.[4] That is, if flux penetration occurs when the internal field $H_a/(1-N)$ equals $H_{c1}(T)$, and given a demagnetization factor $N\simeq1-(\pi t/4R)$ (with t being the thickness and R the radius of the assumed disk shape), one expects that $H_{c1}(T)$ and hence T_c-T should decrease with decreasing R. We must conclude that the laser ablation process causes some degradation of the crystal. A related trend is observed in relaxation rates. Thus, for example, the remanence from an applied field of 1 kOe at 4.2 K decays at a normalized rate $(dM_{\rm rem}/d\ \ln t)/M_0=0.3\%$, 0.7%, 2%, and 3% for the largest square and for the successive stages, respectively.

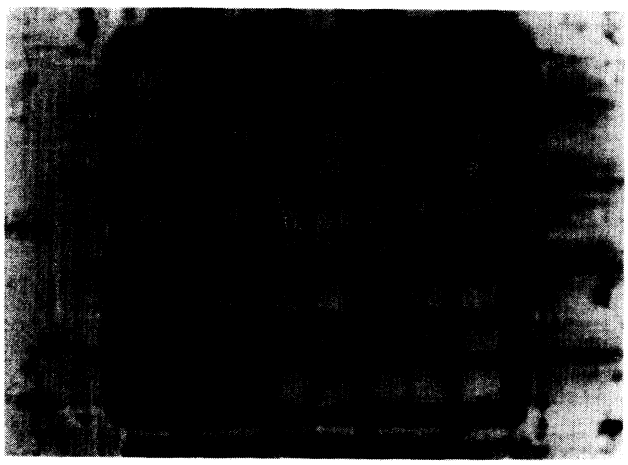

FIG. 1. Last stage of the laser-patterned Y-Ba-Cu-O crystal with 64 40×40 μm^2 isolated squares.

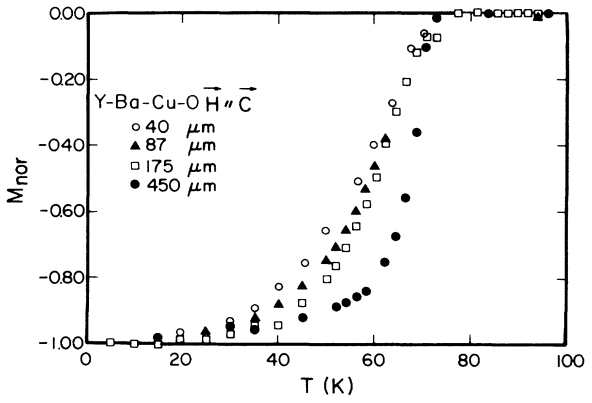

FIG. 2. Temperature dependence of the normalized zero-field-cooled magnetization (**H**||c) for 1, 4, 16, and 64 squares of Y-Ba-Cu-O crystal, measured after application of 50 Oe.

The most informative experiment involves measurements of the $M(H)$ curves at various temperatures. In Fig. 3 are shown the low-temperature (5-K) cycles for **H**||c at the various stages of this experiment. Two features are readily observed in this figure: As the length scale of the squares decreases, (i) the applied field position of the minimum in the virgin curve is almost unshifted (there is only an approximately 25% shift to lower fields in a factor of 5 change in lateral dimension), and (ii) the irreversible magnetization everywhere decreases monotonically. We will return to the minima in Sec. V, but here we consider the scaling of the remanent (zero-field) magnetization in the context of Eq. (1). The remanence increases linearly with size, within experimental error, except for the largest sample, which suggests a sublinear dependence. From Eq. (1), we deduce the apparent J_c, which is proportional to $M_{\rm rem}/R$. In Fig. 4 we present the temperature dependence of $M_{\rm rem}/R$ for the various length scales of this experiment, namely, for the original rectangular sample (denoted by r), for the largest square (denoted by s), and for the subsequent 4-, 16, and 64-

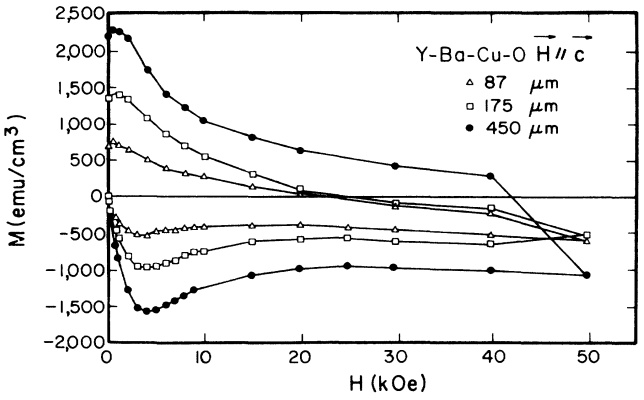

FIG. 3. Low-temperature (5-K) hysteresis curves for **H**||c for 1, 4, 16, and 64 squares of Y-Ba-Cu-O crystal.

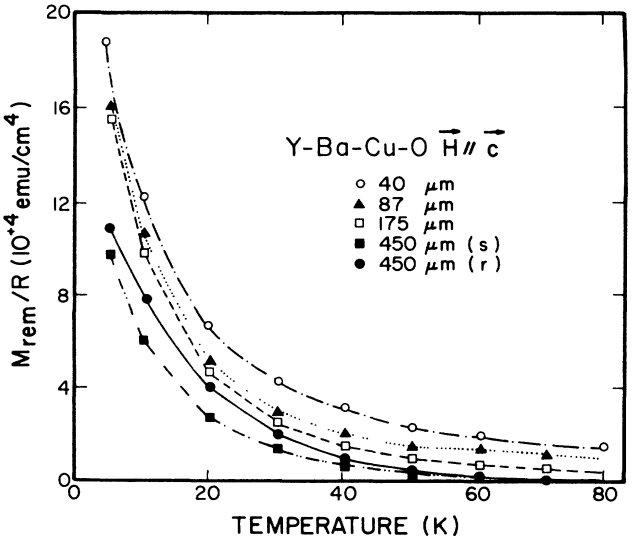

FIG. 4. Values of the dimension-normalized remanent magnetization $M_{\rm rem}/R$ as a function of temperature derived from hysteresis curves with **H**||c for the original rectangular sample (r) and for the subsequent 1, 4, 16, 64 squares of Y-Ba-Cu-O.

square samples. Qualitatively, all five curves exhibit the familiar fast decrease of J_c with temperature, found in magnetic measurements.[21–23] However, it is apparent from Fig. 4 that the calculated values of J_c increase as the length scale decreases, weakly at low temperature, but ever more strongly at high temperature.

Similar experiments to those described in preceding paragraphs for **H**||c were done for **H**⊥c. For magnetic measurements with **H**⊥c, the patterning has no effect on the width of the transition. For a relaxation experiment with **H**⊥c, the normalized relaxation rate is 0.8–1 % for all stages. In Fig. 5, we show the temperature depen-

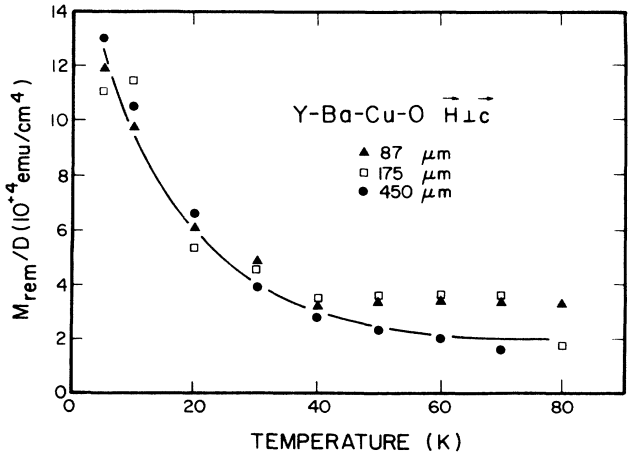

FIG. 5. Values of dimension-normalized remanent magnetization $M_{\rm rem}/D$ as a function of temperature derived from hysteresis curves for **H**⊥c and various length scales D of Y-Ba-Cu-O.

dence of M_{rem} for $\mathbf{H} \perp \mathbf{c}$, normalized to $t \simeq 14$ μm, for the four stages of patterning. The measured values of the remanent magnetization for this configuration are smaller than for $\mathbf{H} \| \mathbf{c}$; as a result of the small signal, the measured values are relatively scattered. Within experimental error, however, Fig. 5 demonstrates that, in accordance with Eq. (2), the patterning has no effect on magnetic measurements when the field is in the plane.

At first glance, this result seems straightforward because, in this configuration, one might have expected the relevant length scale to be the thickness t (approximately 14 μm) of the crystal, independent of the patterning. Actually, recent measurements of critical current anisotropy[8,24,25] in both Y-Ba-Cu-O and Bi-Sr-Ca-Cu-O indicate a different result: except for extremely flat geometries, the critical current density perpendicular to the Cu-O planes is so much weaker than that parallel to the planes that the perpendicular currents dominate the magnetization and are expected to contribute in proportion to the long dimension of the sample. We speculate that in our Mg-doped Y-Ba-Cu-O crystal, the anisotropy must be significantly less than in the samples studied heretofore; this will require further work to confirm.

IV. Bi-Sr-Ca-Cu-O

The ac-susceptibility measurements of the $1300 \times 1300 \times 16$ μm^3 $Bi_{2.15}Sr_{1.65}CaCu_2O_4$ crystal exhibit a broad transition (approximately 5 K) with an onset at $\simeq 78$ K. The original sample was patterned to form 4 and 16 isolated rectangular segments of typical dimensions 500×600 and 200×240 μm, respectively. In contrast to the patterning of the Y-Ba-Cu-O crystal, the ablation has a visible effect on the quality of the Bi-Sr-Ca-Cu-O sample. In particular, many cracks show up on the surface and small areas are spalled off the sample. In the last stage (16 segments), the center grid blocks contained shiny material, giving the appearance of missing grid segments when observed under an optical microscope. However, a qualitative microprobe analysis in a scanning electron microscope (SEM) shows Bi, Sr, and Ca peaks; Cu may have been blocked by the overlying material. We therefore conclude that crystal layers in these "missing" segments were cleaved and spalled off the sample, while the lower layers, in particular those cemented to the sample holder, were left untouched. An enlarged SEM picture of two grid pieces is shown in Fig. 6. Note the appearance of a thin, particle-covered layer, peeling off in sections from the underlying material. During laser patterning, ablated material is redeposited onto nearby segments. By electron microprobe analysis (EMPA) technique, we have found that the ratio of the elements in the cover layer was approximately the same as in the original material. Also, measurements taken at the center and edge of these grids did not indicate any obvious differences in concentrations within each piece.

In Fig. 7 we show the 6-K hysteresis curves for the three length scales of the Bi-Sr-Ca-Cu-O crystal for $\mathbf{H}$ perpendicular to the a-b plane. As in Y-Ba-Cu-O, M_{rem} depends linearly on the length scale, within experimental error, except at the largest size. A similar behavior persists at higher fields.

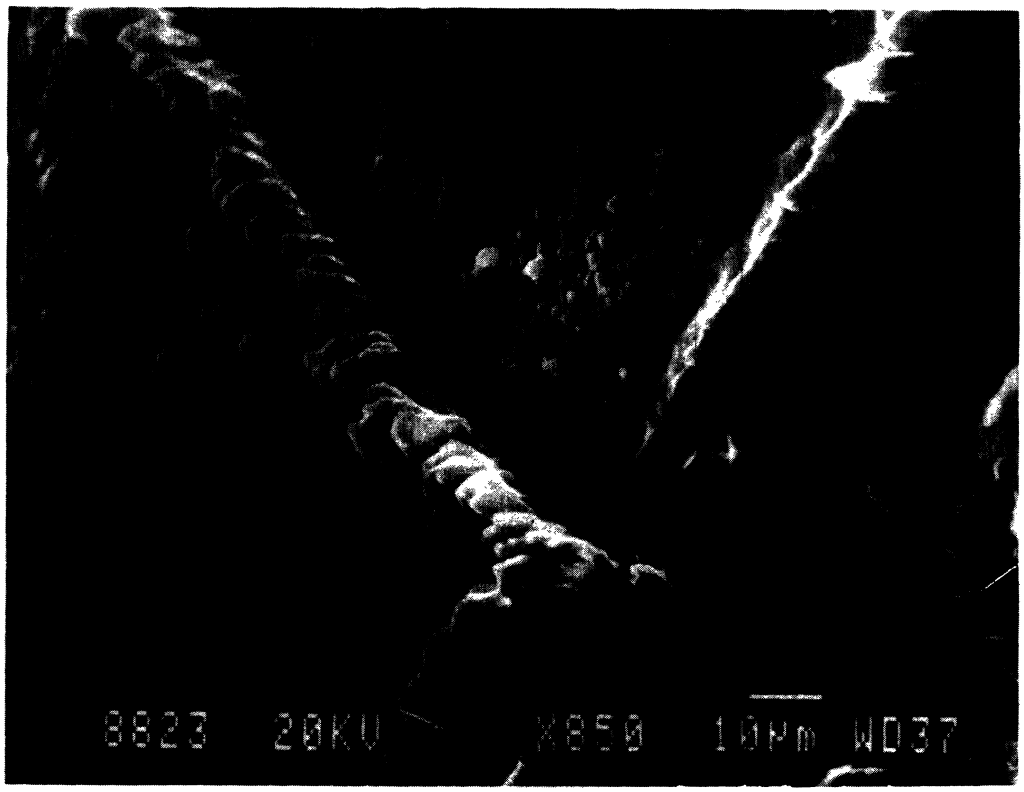

FIG. 6. SEM micrograph of a segment of the patterned Bi-Sr-Ca-Cu-O crystal showing the sidewalls of a laser-ablated trench.

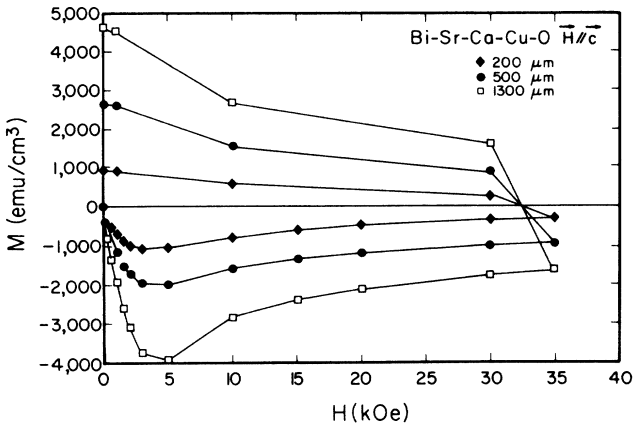

FIG. 7. Low-temperature (6-K) hysteresis curves with H||c for the various length scales of the patterned Bi-Sr-Ca-Cu-O crystal.

V. DISCUSSION

Figures 8(a) and 8(b) plot the size dependence of the low-temperature zero-field remanent magnetization, along with a comparison to a linear and $D^{2/3}$ dependence, for the Y-Ba-Cu-O and Bi-Sr-Ca-Cu-O experiments, respectively. While the $D^{2/3}$ describes the rollover at the largest size, the data follow the linear dependence better at the smaller sizes. At higher temperature, the nonlinearity becomes more pronounced, but here we focus primarily on the low-temperature data.

Granular models for high-temperature superconductors have been widely discussed (e.g., see Ref. 5 for a summary), but they predict a remanent magnetization independent of the exterior length scale. Thus the foremost result of our work is to confirm, in agreement with earlier thin-film work, that good-quality Y-Ba-Cu-O crystals are not granular, at least at low temperatures, at low fields, and at length scales smaller than the 40 μm we have probed. In particular, our data appear to exclude the possibility that twin boundaries, which exist in these crystals on a scale of micrometers, limit the current density at low temperatures.

Nevertheless, the size dependence does not follow the linear prediction of Eqs. (1) and (2) beyond a few hundred micrometers. First, we explore a possible interpretation of this nonlinearity, based on the field dependence of J_c, whose impact on the remanent magnetization has been emphasized recently by Ravi-Kumar and Chaddah.[7] If J_c drops with increasing local flux density h, the remanent flux contour will be flattened, as compared to the triangular flux contour predicted by the conventional Bean formulation. These flux contours are illustrated in Fig. 9. The relative degree of flattening will increase as the sample size increases, leading to a sublinear dependence of remanent magnetization on R.

To calculate this effect we need a phenomenological form for the field dependence of J_c. Among the variety which have been proposed[3,6,7,10] for high-temperature superconductors, we choose a power-law dependence $J_c=\alpha/h^n$ and neglect H_{c1}. The resulting remanent magnetization versus field, ignoring demagnetizing effects

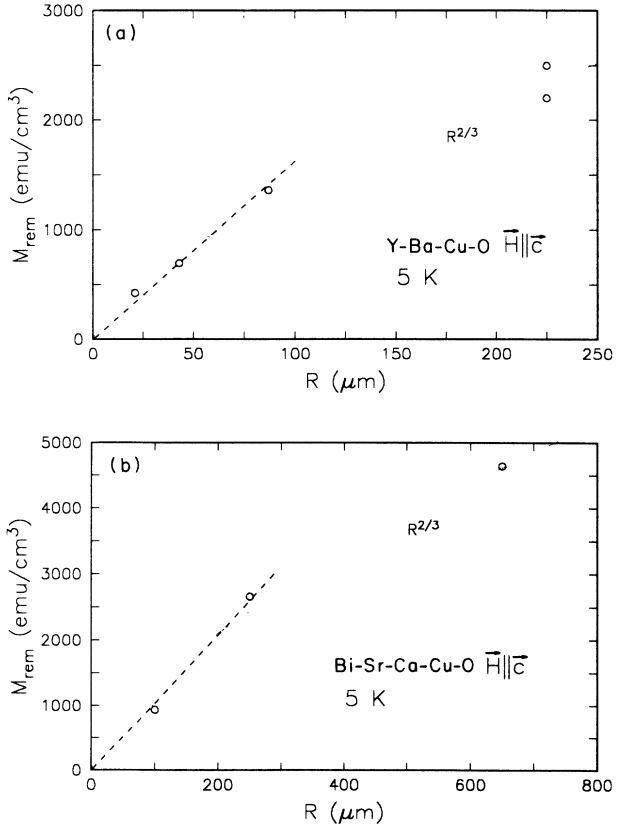

FIG. 8. Remanent magnetization at 5 K as a function of the length scale R (half the square dimension) for (a) Y-Ba-Cu-O and (b) Bi-Sr-Ca-Cu-O. Dotted line represents an $R^{2/3}$ dependence, while the dashed line emphasizes the plausibility of a linear dependence at low sizes.

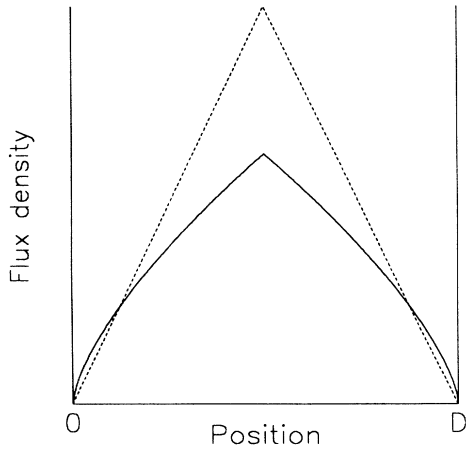

FIG. 9. Sketch of the flux contours in a slab of thickness D after switching off a field sufficient to achieve saturation of the flux density in the sample. The dashed line describes contours for J_c independent of field and solid line describes contours for the field-dependent J_c of Eq. (A1).

(but see below), is calculated in Appendix A. A fit of Eq. (A5) to the data versus field (again, with no demagnetization correction) gives an optimum power n of $\frac{1}{2}$, in agreement with some earlier studies.[3,26–28] on high-T_c materials.

The remanence in this model is predicted to go as R to the power $1/(n+1)$ [see Eqs. (A3) and (A4)]. Thus we immediately obtain the correct power $\frac{2}{3}$ observed in Fig. 8. The fit implies a value for the parameter $\alpha \simeq 4\times 10^8$ (practical units). For example, at a field of 1000 Oe, near the lower critical field, where the $J_c(h)$ dependence might be expected to saturate (rather than diverging as $h\rightarrow 0$ according to the above phenomenological form), J_c attains a value of about 1×10^7 A/cm^2. This is larger than typical values reported in the literature for Y-Ba-Cu-O crystals. Recall, however, that J_c is usually derived with the assumption that $M_{\rm rem}\propto R$ and in our case, Eq. (1) would give 4.5×10^6 A/cm^2. It is apparent from Fig. 9 that this assumption underestimates the value of J_c.

With increasing temperature, Fig. 4 shows more extreme deviation of the remanent magnetization from linearity with size. This effect can possibly be understood in the following way: It is known from earlier work[21,29] that the critical current density depends ever more strongly on field with increasing temperature. This effect can be modeled by taking the power n of the assumed J_c dependence on field to increase with temperature. Since the size dependence goes as $R^{1/(n+1)}$, it is predicted to weaken with temperature, as observed. This picture also offers a possible explanation of why thin-film results show linearity: Their higher J_c's also correspond to weaker dependence of J_c on h.

This interpretation would be on solid ground if the demagnetizing factor of the samples were small. However, the demagnetizing factors N are in fact large, ranging from 0.91 to 0.64 for our Y-Ba-Cu-O experiment, in the approximation of an inscribed ellipsoid. An initially appealing but naive approach to deal with this effect (see Ref. 6 and Appendix B) would be simply to correct the internal field by the *average* demagnetizing field $-4\pi NM$. In this case, the variation in the internal flux density in the critical state is of order J_cR. But Daeumling and Larbalestier[30] have recently shown that a critical-state current distribution in a flat disk (i.e., uniform circulation around the disk) leads to a very different flux distribution. They found that through most of the disk (except at the very center and perimeter), the flux distribution is essentially independent of the sample shape in the limit of a very flat disk ($t \ll R$). That is, the local flux density is a function only of the radial position r normalized by the full radius of the sample. Furthermore, the magnitude of the local flux density scales as J_c, the assumed current density circulating around the disk, times the *thickness* t. These effects are connected with the extreme bending of the flux contours into the disk's plane. The bending is a necessary electromagnetic consequence of the assumed current distribution, creating a critical-state flux gradient which is larger by a ratio R/t along the thickness of the sample than along its diameter. The radially oriented flux density at the surfaces is independent of radius over most of the surface.

Now let us consider[31] how this flux configuration might be affected by a field dependence of J_c. The field dependence will cause the current to be redistributed. In particular, the radially oriented flux density, with its gradient through the thickness, will cause a redistribution through the thickness. Since this component is independent of radius, the average current density associated with it will also be independent of radius. On the other hand, the axially oriented component is relatively small compared to what is assumed in the naive picture (using the average demagnetizing field $-4\pi NM$; see Appendix B). Therefore, the redistribution of the current density along the radius can be expected to be much less than in the naive picture. To the extent that this component can be neglected, the radial distribution will be fully uniform, and in this case it is obvious that the moment will remain linear with radius R. Then Eq. (1) applies, with J_c to be interpreted as an average over the thickness of the sample. Numerical calculations are needed to establish how accurately this simple limit is approached.

This argument undercuts the proposed mechanism for size nonlinearity based on the field dependence of J_c. It suggests that in the platelet or flat-disk geometry, the original simple Bean prediction[1] Eq. (1) is remarkably robust, even in the presence of a field-dependent J_c. This also solves a paradox which emerges from the "naive" critical-state model; namely, that a field-dependent J_c necessarily implies a sublinear dependence of the remanent moment on size (see Appendix A). But while experiment evinces the field dependence of J_c through the field dependence of the irreversible magnetization, it shows a linear size dependence, at least at small sizes. This is just what our argument would predict.

Further evidence in support of the Daeumling-Larbalestier flux distribution comes from the minimum in the virgin curves in Figs. 3 and 7. This minimum shifts hardly at all (at most, a 25% decrease) with a factor of 5–6 decrease in lateral dimension. The conventional demagnetizing model (Appendix B) seems a natural starting point, especially since the initial slopes of the experimental virgin curves are in factor-of-2 agreement with those calculated from a simple ellipsoidal approximation, even for these extremely flat sample shapes. Nevertheless, in such a model, the minimum of the virgin curve is predicted to shift approximately as $R^{1/(n+1)}$ [see Appendix B, Eq. (B8)], where n is the same power used above in describing the field dependence of J_c. While there are no numerical calculations of the virgin curve in the Daeumling-Larbalestier picture, it is plausible that full penetration, corresponding roughly to the minimum, is achieved at an applied field comparable to the vertical fields H_z of their critical state, which scale with J_ct (see their Fig. 1). This argument could explain why the minimum hardly shifts in experiment and seems to support the Daeumling-Larbalestier picture for $\mathbf{H}\|\mathbf{c}$ measurements in plateletlike crystals.

While these arguments explain the linearity observed at the smaller sample sizes, they do not address the sublinear behavior evinced by the largest Y-Ba-Cu-O and Bi-Sr-Ca-Cu-O crystals. One possible explanation is that

the laser ablation technique damages the edges of the pieces, introducing new pinning mechanisms and increasing J_c. Such an effect has been claimed in recent studies of Y-Ba-Cu-O thin films patterned by ion milling or chemical etching.[32] As mentioned above, there is also evidence for some damage of the crystals from the laser ablation process. On the other hand, earlier work[33] on thin films had shown that lines as narrow as 1 μm could be patterned by laser ablation without degradation of T_c. But in our case, many more pulses are required to complete the cut, so the damage may be more significant. A second explanation is based on the assumption that some large-scale defects are present in the largest samples, limiting the uniformity of supercurrent flow. This is possible in view of the sensitivity of the samples to mechanical stresses which were applied during the experiment, leading to some onset of cracking when the crystals were even larger than the sizes reported here. This hypothesis is supported by optical observation under crossed polarizers before the patterning, which revealed some changes of contrast on a large scale.

VI. SUMMARY AND CONCLUSIONS

We have developed a new technique for grid-patterning thin high-T_c crystals. We are thus able to measure directly the dependence of the remanent magnetization on the lateral geometrical length scale R. At low temperature we find an essentially linear dependence for Y-Ba-Cu-O and Bi-Sr-Ca-Cu-O crystals, at least at the smaller sizes, confirming Bean's original prediction for the critical-state model. This size dependence appears to rule out strong granularity, for example, on the scale of twin boundaries. At larger sizes (and low temperatures), both crystals show sublinear behavior, indicating some large-scale ($\simeq 100$-μm) features that limit current flow. We have also explored the effect of a field dependence in the critical current density on the remanence. This could explain nonlinearity in samples with small demagnetizing factors, but in our case with large demagnetizing factors, we argue this mechanism most likely does not apply because of the extreme bending of flux lines expected in the critical state.[30] Our data give some evidence for this novel critical state, in which the dominant flux gradient occurs through the thickness of the sample. At higher temperatures, the stronger sublinear behavior suggests the appearance of new obstacles to current flow on an ever-finer scale or else the increasing effect of pinning centers created by the laser cutting process.

ACKNOWLEDGMENTS

It is a pleasure to acknowlege T. Worthington for ac-susceptibility measurements as well as collaboration and discussion throughout this work, M. M. Oprysko for the help with the laser patterning, K. Kelleher for SEM and EMPA measurements, and M. Daeumling, L. Krusin-Elbaum, and C. Tsuei for helpful discussions. Y.Y. and A.P.M. would like to acknowledge partial support from the United States–Israel Binational Science Foundation.

APPENDIX A: EFFECT OF J_c FIELD DEPENDENCE ON REMANENCE

Here we present an extension of the Bean model[1,2] to take into account the field dependence of the critical current density $J_c(h)$ and to calculate the remanence. This has been widely studied in the low-T_c literature,[34–36] and many authors[2,3,6,7,10] have explored such effects in high-temperature superconductors as well. We use a phenomenological form which permits an analytical expression for the size dependence of interest to us. The equations are useful for treating configurations with low demagnetizing factor N. We also use the equations in the text to compare to our results in the high-demagnetizing-factor configuration; we conclude that in spite of an appealing fit to the experimental data, present understanding of the flux configuration makes this interpretation unlikely for $N \rightarrow 1$.

If J_c drops with increasing field, the shape of the flux contours in the Bean model and, as a result, the expressions for the remanent magnetization are modified from those of Eqs. (1) and (2). In Fig. 9 we sketch the field contours in a slab of thickness D, after switching off a sufficiently large applied field to achieve a saturation of the remanence. The dashed lines are the contours assumed in the original Bean model with slope proportional to J_c and independent of local flux density h. The curved solid lines arise from the field dependence of J_c, which we model as[3]

$$J_c = \alpha / h^n , \tag{A1}$$

where α is a constant and n is some power, found to be $\frac{1}{2}$ in some earlier studies of several type-II superconductors,[37,38] and also in the high-temperature superconductors.[26] This form neglects effects associated with the lower critical field, assumed to be small, and is related to the earlier form of Kim and co-workers[39] for the field dependence of J_c by neglecting the field offset. In what follows we will also neglect contributions from the equilibrium magnetization.

The saturation remanent magnetization (in the absence of demagnetizing effects) is given by the volume average

$$4\pi M_{\rm rem} = \left[\int h \, dv \right] \Big/ \int dv \ . \tag{A2}$$

Thus $M_{\rm rem}$ is proportional to the area below the h contour in Fig. 9. It is apparent from this figure that while the area increases linearly with D for the original Bean model (i.e., for J_c independent of h), the increase is slower for the solid lines which curve further down as D increases. Integrating, we find

$$4\pi M_{\rm rem} = \frac{2(n+1)^{(2n+3)/(n+1)}}{(n+2)(2n+3)} \left[\frac{2\pi\alpha R}{5} \right]^{1/(n+1)} , \tag{A3}$$

$$4\pi M_{\rm rem} = \frac{(n+1)^{(n+2)/(n+1)}}{(n+2)} \left[\frac{\pi\alpha D}{5} \right]^{1/(n+1)} , \tag{A4}$$

for a cylinder of radius R and a slab of thickness D, respectively. Note that for $n=0$, Eqs. (1) and (2) are recovered. Equations (A3) and (A4) predict that $M_{\rm rem}$ is

proportional to a power $1/(n+1)$ of the length scale. The linear relationship is expected only for the case $n=0$.

Within the same model, it is of course possible to calculate the full hysteresis loop, as has been done[6,7,10] for other phenomenological forms of $J_c(h)$. In particular, when the applied field H is decreasing from a sufficiently high value to achieve saturation, we find for a cylinder of radius R

$$4\pi M=-H+\frac{25}{2\pi^2\alpha^2R^2}\left[K\frac{K^{(n+2)/(n+1)}-H^{n+2}}{(n+1)(n+2)}-\frac{K^{(2n+3)/(n+1)}-H^{2n+3}}{(n+1)(2n+3)}\right], \tag{A5}$$

with

$$K\equiv H^{n+1}+\frac{2\pi(n+1)\alpha R}{5}. \tag{A6}$$

Similarly, for a slab of thickness D

$$4\pi M=-H+\frac{5}{(n+2)\pi\alpha D}\times\left[\left[H^{n+1}+\frac{(n+1)\pi\alpha D}{5}\right]^{(n+2)/(n+1)}-H^{n+2}\right]. \tag{A7}$$

Equations (A5)–(A7) reduce to Eqs. (A3) and (A4) when $H=0$, and predict a field-independent irreversible magnetization for $n=0$.

APPENDIX B: DEMAGNETIZATION IN THE CRITICAL STATE

We investigate here the effect of a finite (ellipsoidal) demagnetization factor N on the magnetic response of a type-II superconductor, in the context of an extended Bean model with a power-law dependence for the critical current density [Eq. (A1)]. These results should be useful for the case of low demagnetizing factors. In the case of large demagnetizing factors ($N\rightarrow 1$), there are major corrections to this simple picture, as pointed out recently by Daeumling and Larbalestier.[30] Nevertheless we give some results of the "naive" treatment for $N\rightarrow 1$ in the interest of providing a contrast to the predictions of the more complete theory and a basis for testing these models in experiment. Since the conventional naive model underlies so much of the past thinking about these materials, it is important to test it and prove experimentally that it really is inapplicable.

Since the critical state generates a nonuniform magnetization through the sample, it violates the conditions for a conventional treatment of demagnetization for ellipsoidal samples. This is the essential problem in the case $N\rightarrow 1$. Nevertheless, the natural first approximation,[6] which is reasonable for low N, is to calculate the magnetization from the current distribution, then to *assume* that magnetization is uniform, and finally to calculate self-consistently the internal field H_i as

$$H_i=H_a-4\pi NM, \tag{B1}$$

where H_a is the applied field.

Let us calculate the initial penetration of the flux (the "virgin curve") in such a model. For simplicity we use a flat ribbon of width D and thickness t with applied field perpendicular to the plane. The local flux-density contour as a function of position x from the edge is

$$h(x)=[H_i^{n+1}-2\pi(n+1)\alpha x/5]^{1/(n+1)}. \tag{B2}$$

Integrating over position and dividing by D, we obtain the magnetization

$$4\pi M=-H_i+5H_i^{n+2}[\pi(n+2)\alpha D]^{-1}, \tag{B3}$$

applicable for $0<H_i<[\pi(n+1)\alpha D/5]^{1/(n+1)}$. Along with Eq. (B1), this implicitly determines the magnetization as a function of applied field and demagnetizing factor.

The case $n=0$ is of particular interest because it applies when the current density is essentially independent of induction across the sample, which occurs in ac susceptibility measurements in a large dc field. Here we can solve for $4\pi M$ explicitly:

$$4\pi M=\frac{-H^*(N-1)+H_aN-[H^{*2}(1-N)^2+2NH^*H_a]^{1/2}}{N^2}, \tag{B4}$$

where $H^*\equiv\pi J_{c0}D/5$ [$J_{c0}\equiv\alpha$ for $n=0$ in Eq. (A1)] and H_a can be interpreted as the small ac field. Starting from zero, the magnetization increases with the expected slope $-1(1-N)$, which extrapolates to the saturation value of $H^*/2$ at $H_{\rm extrap}=H^*(1-N)/2$. Then it curves over to reach its saturation value at $H_{\rm sat}-H^*(1-0.5N)$, where th flux contours meet in the center of the sample. This makes clear the meaning of H^*: It is the field of saturation *when* $N=0$ (and $n=0$). The slope at the saturation point is zero, as can be confirmed from the differential susceptibility $\chi\equiv dM/dH_a$:

$$4\pi\chi=N^{-1}\{1-H^*[H^{*2}(1-N)^2+2NH^*H_a]^{-1/2}\}, \tag{B5}$$

and this makes the saturation point difficult to pick out experimentally.

In the limit of the large demagnetization factor for a long flat slab, where $1-N\rightarrow 1-(t/D)$, these results are interesting because the field intercept reduces from the above formulas to

$$H_{\rm extrap}=H^*(1-N)/2=\pi Jt/10, \tag{B6}$$

even though the true saturation point is

$$H_{\rm sat}=H^*\left[1-\frac{N}{2}\right]\simeq\pi JD/5\ . \tag{B7}$$

That is, the *apparent* (extrapolated) intercept field scales with t even though the true intercept at saturation scales with D. This is of particular importance because Daeumling and Larbalestier[30] argue that a more appropriate model gives a saturation field (which they call h^*) scaling as Jt. Since the true saturation point in our conventional model occurs at a point of zero slope, it is hard to pick out (and may also be in the Daeumling-Larbalestier picture), and therefore it may be difficult to distinguish between these pictures in comparing to such experiments.

A more promising approach for distinguishing these pictures is to consider the field dependence of the differential susceptibility χ. According to Eq. (B5), χ rises from $-1(1-N)$ with a slope $4\pi d\chi/dH_a$ of $[H^*(1-N)^3]^{-1}$, which can be extrapolated to intersect 0 at $H^*(1-N)^2$ or $\pi Jt^2/5D$; this should be testable in experiment. The true saturation field is still difficult to identify because the slope $(1/H^*)$ is still small.

Finally, we return to the more general model with $n\neq 0$ to calculate the minimum in the magnetization of the virgin curve. Taking the applied-field derivative of Eqs. (B1) and (B3), we find

$$H_{a,\rm min}=\left[1-N\frac{n+1}{n+2}\right]\left[\frac{\pi\alpha D}{5}\right]^{1/(n+1)}, \tag{B8}$$

at which point

$$4\pi M_{\rm min}=-\frac{n+1}{n-2}\left[\frac{\pi\alpha D}{5}\right]^{1/(n+1)}. \tag{B9}$$

Thus, for $n>0$ and N close to 1, $H_{a,\rm min}$ depends only weakly on the demagnetizing factor N and scales approximately as $D^{1/(n+1)}$, a conclusion which conflicts with experiment. As discussed in the text, this discrepancy adds evidence that there is a basic problem in the assumptions of the conventional demagnetizing model we have used in this section, at least when $N\rightarrow 1$.

---

*Permanent and present address: Department of Physics, Bar-Ilan University, Ramat-Gan, 52100, Israel.

†Permanent and present address: IBM Zürich Research Laboratory, 8803 Rüschlikon, Switzerland.

[1]C. P. Bean, Phys. Rev. Lett. **8**, 250 (1962); Rev. Mod. Phys. **36**, 31 (1964).

[2]A. M. Campbell and J. E. Evetts, Adv. Phys. **21**, 199 (1972).

[3]Y. Yeshurun, A. P. Malozemoff, F. Holtzberg, and T. R. Dinger, Phys. Rev. B **38**, 11 828 (1988).

[4]L. Krusin-Elbaum, A. P. Malozemoff, Y. Yeshurun, D. C. Cronemeyer, and F. Holtzberg, Phys. Rev. B **39**, 2936 (1989).

[5]A. P. Malozemoff, in *Physical Properties of High Temperature Superconductors I,* edited by D. M. Ginsberg (World Scientific, Singapore, 1989), p. 71, and references therein.

[6]H. Dersch and G. Blatter, Phys. Rev. B **38**, 11 391 (1988).

[7]G. Ravi-Kumar and P. Chaddah, Phys. Rev. B **39**, 4704 (1989); P. Chaddah, K. V. Bhagwat, and G. Ravikumar, Physica C (to be published).

[8]E. M. Gyorgy, R. B. van Dover, K. A. Jackson, L. F. Schneemeyer, and J. V. Waszczak, Appl. Phys. Lett. **55**, 283 (1989).

[9]R. L. Peterson, Phys. Rev. B **40**, 2678 (1989).

[10]V. V. Moshchalkov *et al.* (unpublished); V. V. Moshchalkov, O. V. Petrenko, V. S. Belov, and V. I. Voronkova, Physica C **162–164**, 1633 (1989).

[11]B. Oh, M. Naito, S. Arnason, P. Rosenthal, R. Barton, M. R. Beasley, T. H. Geballe, R. H. Hammond, and A. Kapitulnik, Appl. Phys. Lett. **51**, 852 (1987).

[12]T. R. McGuire, D. Dimos, R. H. Koch, R. B. Laibowitz, and J. Mannhart, IEEE Trans. Magn. **25**, 3218 (1989); and (private communication).

[13]J. Mannhart, M. Scheuermann, C. C. Tsuei, M.. M. Oprysko, C. C. Chi, C. P. Umbach, R. H. Koch, and C. Miller, Appl. Plys. Lett. **52**, 1271 (1988).

[14]A. Sulpice, P. Lejay, R. Tournier, and J. Chaussy, Europhys. Lett. 7, 365 (1988).

[15]H. Küpfer, I. Apfelstedt, R. Flükiger, C. Keller, R. Meier-Hirmer, B. Runtsch, A. Turowski, U. Weich, and T. Wolf, Cryogenics **28**, 650 (1988).

[16]A. D. Hibbs and A. M. Campbell, IEEE Trans. Magn. **25**, 2142 (1989).

[17]M. Daeumling, J. Seuntjens, and D. C. Larbalestier, Appl. Phys. Lett. **52**, 590 (1988).

[18]E. Shimizu and D. Ito, Phys. Rev. B **39**, 2921 (1989).

[19]D. L. Kaiser, F. H. Holtzberg, M. F. Chisholm, and T. K. Worthington, J. Cryst. Growth. **85**, 593 (1987).

[20]G. V. Chandrashekhar and M. W. Shafer (unpublished).

[21]T. R. Dinger, T. K. Worthington, W. J. Gallagher, and R. L. Sandstrom, Phys. Rev. Lett. **58**, 2687 (1987).

[22]Y. Yeshurun, A. P. Malozemoff, and F. Holtzberg, J. Appl. Phys. **64**, 5797 (1988).

[23]S. Senoussi, M. Oussena, G. Collin, and I. A. Campbell, Phys. Rev. B **37**, 9792 (1988).

[24]B. D. Biggs, M. N. Kunchur, J. J. Lin, S. J. Poon, T. R. Askew, R. B. Flippen, M. A. Subramanian, J. Gopalakrishnan, and A. W. Sleight, Phys. Rev. B **39**, 7309 (1989).

[25]D. C. Cronemeyer, T. R. McGuire, A. P. Malozemoff, F. Holtzberg, R. J. Gambino, L. W. Conner, and M. W. Meelfresh, in *Proceedings of the International Conference on Transport Properties of Superconductors,* edited by R. Nicolsky (World Scientific, Singapore, to be published).

[26]P. Kes, Physica C **153-155**, 1121 (1988).

[27]Y. Wolfus, Y. Yeshurun, I. Felner, and H. Sompolinsky, Phys. Rev. B **40**, 2701 (1989).

[28]L. Ji, R. H. Sohn, G. C. Spalding, C. J. Lobb, and M. Tinkham, Phys. Rev. B **40**, 10 936 (1989).

[29]D. E. Farrell, B. S. Chandrasekhar, M. R. DeGuire, M. M. Fang, V. G. Kogan, J. R. Clem, and D. K. Finnemore, Phys. Rev. B **36**, 4025 (1987).

[30]M. Daeumling and D. C. Larbalestier, Phys. Rev. B **40**, 9350 (1989).

[31]M. Daeumling (private communication); L. W. Conner and A.

P. Malozemoff, Phys. Rev. B (to be published).
[32]S. Tahara, S. M. Anlage, C.-B. Eom, D. K. Fork, T. H. Geballe, and M. R. Beasley, Physica C **162-164**, 1175 (1989).
[33]J. Mannhart, P. Chaudhari, D. Dimos, C. C. Tsuei, and T. R. McGuire, Phys. Rev. Lett. **61**, 2476 (1988).
[34]W. I. Dunn and P. Hlawiczka, J. Phys. D **1**, 1469 (1968); M. Green and P. Hlawiczka, Proc. IEE **114**, 1329 (1967).
[35]F. Irie and K. Yamafuji, J. Phys. Soc. Jpn. **23**, 255 (1967).
[36]J. A. Hulbert, J. Phys. D **16**, 1657 (1965).
[37]K. Yasukochi, T. Ogasawara, N. Usui, H. Kobayashi, and S. Ushio, J. Phys. Soc. Jpn. **19**, 137 (1964); **21**, 89 (1966).
[38]M. A. R. LeBlanc, G. Fillion, and J. P. Lorrain, J. Appl. Phys. **59**, 3208 (1986).
[39]P. W. Anderson and Y. B. Kim, Rev. Mod. Phys. **36**, 39 (1964); Y. B. Kim, C. F. Hempstead, and A. R. Strnad, *ibid.* **36**, 43 (1964).

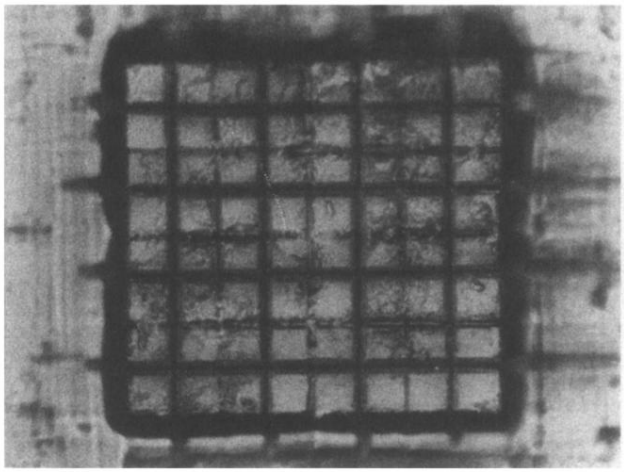

FIG. 1. Last stage of the laser-patterned Y-Ba-Cu-O crystal with 64 $40 \times 40\ \mu m^2$ isolated squares.

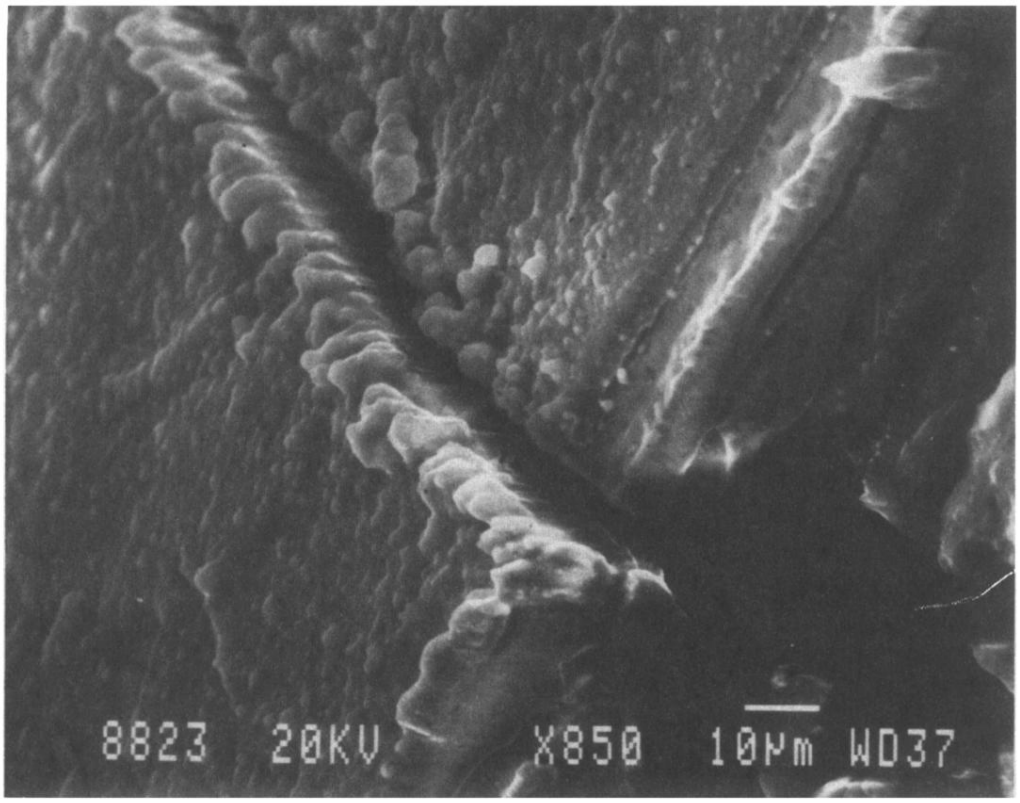

FIG. 6. SEM micrograph of a segment of the patterned Bi-Sr-Ca-Cu-O crystal showing the sidewalls of a laser-ablated trench.